21st European Workshop on White Dwarfs
Castanheira, Vanderbosch, Montgomery, eds.
July 23–27, 2018, Austin, Texas, USA

The *Gaia* white dwarf population within 100 pc of the Sun

S. Torres,[1,2] A. Rebassa-Mansergas,[1,2] F. M. Jiménez-Esteban,[3,4] C. Cantero,[1] P. Canals[1], G. Skorobogatov[1] and E. Solano[3,4]

[1] *Departament de Física, Universitat Politécnica de Catalunya, c/Esteve Terrades 5, 08860 Castelldefels, Spain; santiago.torres@upc.edu*
[2] *Institut d'Estudis Espacials de Catalunya, Ed. Nexus-201, c/Gran Capitá 2-4, 08034 Barcelona, Spain*
[3] *Departmento de Astrofísica, Centro de Astrobiología (CSIC-INTA), ESAC Campus, Camino Bajo del Castillo s/n, E-28692 Villanueva de la Cañada, Madrid, Spain*
[4] *Spanish Virtual Observatory, Spain*

Abstract

The recent *Gaia* Data Release 2 has provided an unprecedented sample of the local white dwarf population. The high astrometric resolution and the photometry provided by *Gaia* allows to build a clean magnitude-color diagram that, with the aid of the most updated population synthesis simulator, permit us to select the sample of white dwarf candidates. Our analysis shows that *Gaia* has virtually identified all white dwarfs within 100 pc from the Sun. Additionally, we use the Virtual Observatory tool VOSA to derive effective temperatures and luminosities for our sources by fitting their spectral energy distributions. The *Gaia* 100 pc white dwarf population is clearly dominated by cool ($\sim$8,000 K) objects and reveals a significant population of massive ($M \sim 0.8 M_{\odot}$) white dwarfs, of which no more than $\sim 30 - 40\,\%$ can be attributed to hydrogen-deficient atmospheres. Preliminary results including white dwarf mergers seem not to explain this excess unless some *ad hoc* hypothesis are adopted. Finally, we use an Intelligent Artificial algorithm based on the Random Forest method to disentangle the different Galactic components of the white dwarf population. Our results show that the thin, thick and halo ratio in the 100 pc sample is 89:11:1, identifying 97 halo white dwarf candidates.

1 The Population Synthesis Simulator

With the aid of a detailed population synthesis code we build a thorough sample model of the local Galactic white dwarf population. Our synthetic sample allow us to define the regions within the *Gaia* HR-diagram where we expect to identify white dwarfs, as well as to predict its completeness and to analyze its parameter distributions. Our population synthesis code, based on Monte Carlo techniques, has been widely used in the study of the white dwarf population of the different components of the Galaxy, as well as in globular and open clusters (García-Berro et al., 1999; García-Berro et al., 2010; Torres et al., 2001; Torres et al., 2015; Torres & García-Berro, 2016, and references therein). In particular, a comprehensive study of the capabilities of *Gaia* and previous estimates of the Galactic white dwarf population can be found in Torres et al. (2005). In what follows we briefly describe the main ingredients employed in our simulations, where a detailed description and references can be found in Jiménez-Esteban et al. (2018).

The white dwarf population is simulated according to a three-component Galactic model: thin and thick disk, and halo. For the thin disc population, we adopt an age of 9.2 Gyr with a constant star formation rate, while the spatial distribution of the synthetic stars follows a double exponential profile with a scale height of 250 pc and a scale length of 2.6 kpc. The thick disc is modeled from a star formation rate peaked at 10 Gyr in the past and extended up to 12 Gyr. Similarly, the thick disc population follows a double exponential spatial distribution but with a scale height of 1,500 pc and a scale length of 3.5 kpc. The born time for synthetic stars of the halo population is randomly assigned within a burst of constant star formation lasting 1 Gyr that happened 13.5 Gyr in the past. Besides, halo stars are located according to an isothermal distribution. Kinematic properties of each Galactic component are drawn according to the observed estimates by Rowell & Hambly (2011). The mass of main-sequence stars are randomly chosen following a Salpeter-like initial mass function with $\alpha = -2.35$.

Once we determine which stars have become white dwarfs, we evaluate their cooling evolution by means of an updated set of white dwarf evolutionary cooling

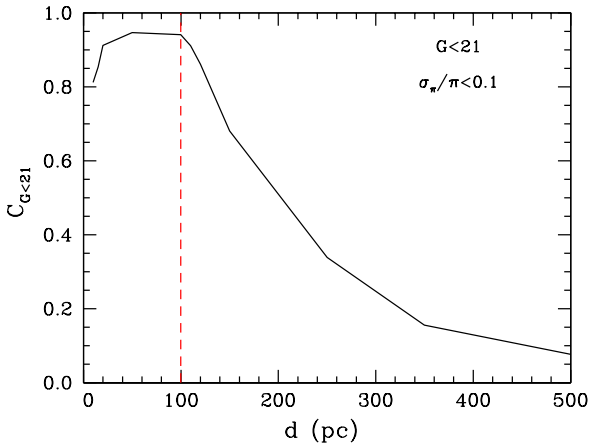

Figure 1: Completeness of our synthetic *Gaia* white dwarf sample as a function of the distance when the restrictions in G magnitude, $G < 21$, and in relative parallax error, $\sigma_\pi/\pi < 0.1$, are applied. Samples below 100 pc can be practically considered complete volume-limited sample, while above this distance samples shall be considered magnitude-limited.

sequences provided by La Plata Group – see Camisassa et al. (2017); Althaus et al. (2015) and references therein. These sequences are metallicity dependent and encompass the full range of white dwarf masses for CO-core and ONe-core white dwarfs. Additionally, for each of the white dwarfs generated, we consider hydrogen-rich (DA) or hydrogen-deficient atmospheres (non–DA) white dwarfs according to the canonical distribution of 80% DA and 20% non–DA. Colours and magnitudes are then interpolated in the corresponding cooling sequences and transformed to the *Gaia* photometric system. The simulated synthetic population for the three Galactic components is then mixed proportionally to 80:15:5 for the thin disc, thick disc, and halo, respectively. Finally, and in order to mimic the observational procedure, we introduced a photometric and an astrometric error for each of our simulated objects as prescribed in the *Gaia* performances[1].

One of the multiple issues that our population synthesis simulator permit to study is the completeness of the white dwarf population available by *Gaia*. In Figure 1 we show the completeness of our synthetic sample as a function of the distance when the restrictions in G magnitude, $G < 21$, and in relative parallax error, $\sigma_\pi/\pi < 0.1$, are applied. As can be seen in Fig.1 the white dwarf sample available by *Gaia* is practically complete (above a 85%) up to 100 pc, where from here on the completeness dramatically decreases up to a 8% at 500 pc. Consequently, *Gaia* white dwarf samples up to 100 pc can be considered as nearly complete volume-limited samples, while for larger volumes magnitude-limiting effects must be taken into account.

[1]http://www.cosmos.esa.int/web/gaia/science-performance

2 The *Gaia*-DR2 sample

Our population synthesis simulator permit us to establish certain regions of the Hertzsprung-Russell diagram where we expected to find the *Gaia* white dwarf population. In Figure 2 we show these regions. First, we delimit a wide region where all single white dwarfs accessible by *Gaia* can be found (red dashed line). Secondly, we define a region where we expected to find white dwarfs within 100 pc ($M_G > 2.95 \times (G_{\rm BP} - G_{\rm RP}) + 10.83$). Additionally, for the 100 pc sample and imposed by our atmospheric white dwarf models, we delimit a region for effective temperatures within the range 6,000 K< $T_{\rm eff}$ <80,000 K. This is equivalent to add a colour restriction $-0.52 < (G_{\rm BP} - G_{\rm RP}) < 0.80$. The magnitude-colour region thus obtained is marked as red dotted lines in Fig. 2, where the region of the sub-sample of CO-core white dwarfs is marked by a red continuous line box. For illustrative purposes we also show in Fig.2 the theoretical cooling tracks for a typical $0.6\,M_\odot$ CO-core hydrogen-rich atmosphere (Renedo et al., 2010) – blue line –, a $0.6\,M_\odot$ CO-core hydrogen-deficient atmosphere (Camisassa et al., 2017) – magenta line –, and a $1.2\,M_\odot$ ONe-core white dwarf (**?**) – green line. According to our analysis we search for white dwarf candidates in the *Gaia* DR2 catalogue[2] using the following criteria:

- $\pi > 10$ mas and $\pi/\sigma_\pi > 10$
- $F_{\rm BP}/\sigma_{F_{\rm BP}} > 10$ and $F_{\rm RP}/\sigma_{F_{\rm RP}} > 10$
- $phot\_bp\_rp\_excess\_factor < 1.3 + 0.06 \times (G_{\rm BP} - G_{\rm RP})$
- $-0.52 < (G_{\rm BP} - G_{\rm RP}) < 0.80$
- $2.95 \times (G_{\rm BP} - G_{\rm RP}) + 10.83 < M_G < 3.02 \times (G_{\rm BP} - G_{\rm RP}) + 13.18$ for CO-core white dwarfs
- $M_G > 3.02 \times (G_{\rm BP} - G_{\rm RP}) + 13.18$ for ONe-core white dwarfs

The cut in the *phot_bp_rp_excess_factor* prevented against photometric errors in the BP and RP bands, which are especially important for faint sources in crowded areas. In Fig.2 we show the sample thus obtained (black dots), while those objects discarded by an excess of the photometric factor are also plotted (gray dots). The 100 pc *Gaia* white dwarf sample thus derived contains 8,343 CO-core and 212 ONe-core within the range of effective temperatures of 6,000 K< $T_{\rm eff}$ <80,000 K. Once corrected from completeness, we derived from these values a white dwarf spatial density of $4.9 \pm 0.4 \times 10^{-3}$ pc^{-3} for the 100 pc sample. All the relevant information of these sources can be gathered from *The SVO archive of Gaia white dwarfs* at the Spanish Virtual Observatory portal[3] and the full analysis is presented in Jiménez-Esteban et al. (2018).

[2]http://gea.esac.esa.int/archive/
[3]http://svo2.cab.inta-csic.es/vocats/v2/wdw

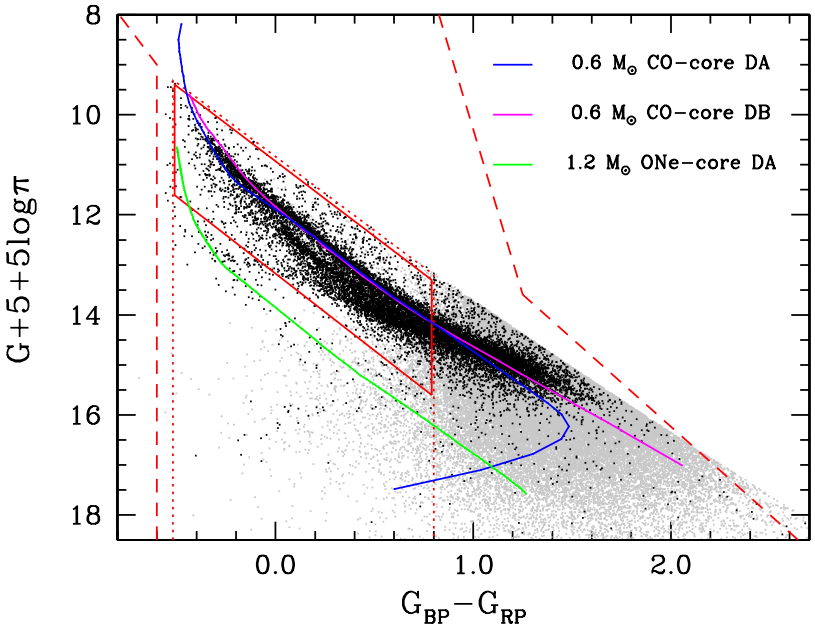

Figure 2: *Gaia* G absolute magnitude - colour diagram for the *Gaia* white dwarf population within 100 pc. Those objects that do not fulfill our colour excess criterion are marked as gray dots. Theoretical cooling tracks for a typical $0.6\,M_{\odot}$ (and $1.2\,M_{\odot}$) white dwarf with different composition are shown with solid lines. The dashed lines define the region where all single white dwarfs accessible by *Gaia* were expected to be found. The dotted box delimit the region for those objects within 100 pc and within our effective temperature range, while those with CO-cores are delimited by the solid red line box (see text for details).

3 Deriving Parameters

In order to derive the physical parameter of the objects of our *Gaia* sample, we take advantage of VOSA[4] (Bayo et al., 2008) tool. VOSA is a Virtual Observatory tool designed to determine physical parameters (such as effective temperature and luminosity) of thousands of objects at once. VOSA compares observed photometry, gathered from a significant number of VO complaint catalogues, to different collections of theoretical models. This way we build the observational SEDs from the UV to the NIR wavelength range, where white dwarfs mainly radiate their light. The observational SEDs are then compared to a grid of synthetic spectra specifically developed for white dwarfs. In particular we adopted an updated DA white dwarf model spectra of Koester (2010) for effective temperatures ranging from 5,000 K to 80,000 K. Two physical parameters are obtained from the SED fitting: effective temperature and luminosity. This last is obtained from the bolometric flux and the distance obtained from the *Gaia* parallax. To calculate the bolometric flux, VOSA integrates the flux using the observational photometric points, and the theoretical model that best fits at the region of the SEDs not covered by the observations. This allows to obtain a more accurate bolometric flux, and so luminosity, than from bolometric corrections. In addition, the effective temperature is obtained from the SED fitting instead than from the *Gaia* colour, which minimizes the impact of photometric errors at the *Gaia* bands. From the effective temperatures and the luminosities provided by VOSA we derive the radii by using the well known Stefan-Boltzmann law. Finally, we can interpolate the effective temperature and radius values in the evolutionary sequences for DA white dwarfs of Renedo et al. (2010) to obtain their surface gravities and masses.

Among the 8,343 CO-core and 212 ONe-core white dwarfs located within 100 pc from the Sun, the VOSA SED fitting provided reliable results for 52%, i.e. 4,317 CO-core and 88 ONe-core white dwarfs. A complete analysis and discussion of the physical properties of the white dwarf parameters thus obtained can be found in Jiménez-Esteban et al. (2018). Here, we present in Figure 3 the temperature distribution (top panel) and the mass distribution (bottom panel) for 100 pc *Gaia* white dwarf sample (gray solid histogram) compared to our simulated distribution (red open histogram). In general terms, the observed temperature distribution perfectly agrees with the simulated one (top panel of Fig.3). However, there is a clear lack of observed white dwarfs at the coolest temperature range ($T_{\rm eff}$ <8,000 K). This effect can be attributed to the cut in the *phot_bp_rp_excess_factor*, which eliminate objects with large photometric errors in the BP and RP bands, specially for redder colours, i.e. cooler effective temperatures. In any

[4]http://svo2.cab.inta-csic.es/theory/vosa

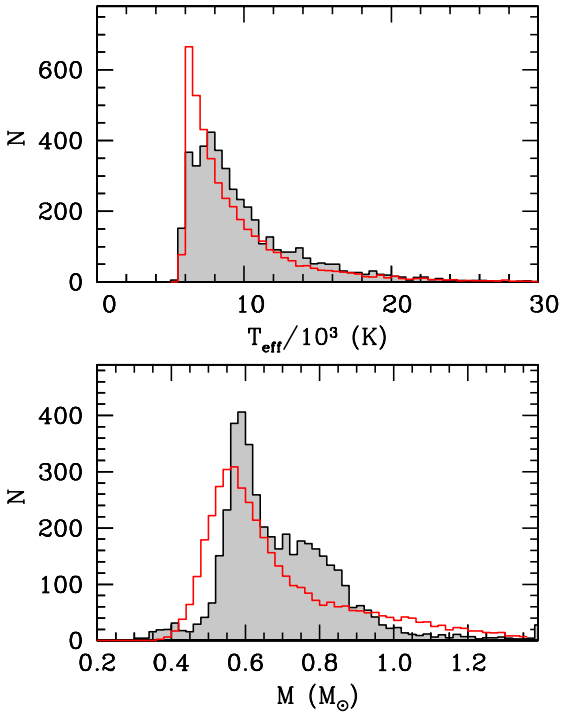

Figure 3: Effective temperature distribution (top panel) and mass distribution (bottom panel) for the 100 pc *Gaia* white dwarf sample (gray solid histogram) compared to our simulated distribution (red open histogram).

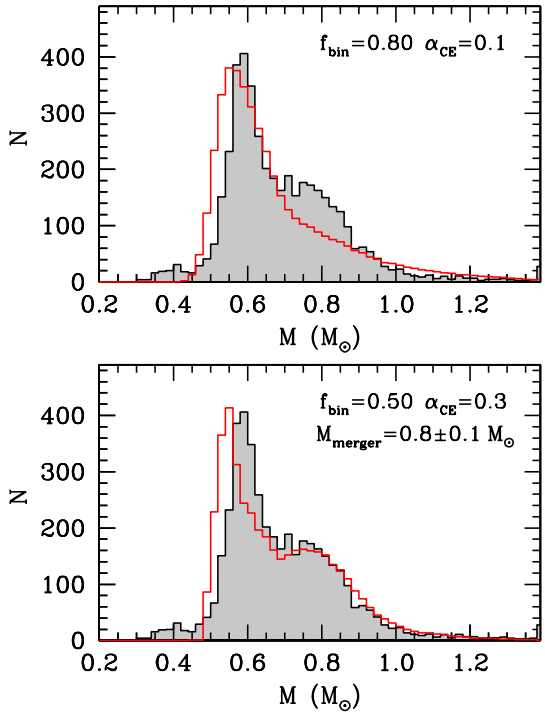

Figure 4: Mass distribution for the 100 pc *Gaia* white dwarf sample (gray solid histogram) compared to our simulated distribution (red open histogram) when a standard binary model which incorporate white dwarf mergers is used (top panel) and when the mass of the white dwarf merger is forced to be $0.8 \pm 0.1\,M_{\odot}$.

case, the temperature distribution obtained clearly demonstrated that the *Gaia* white dwarf sample is dominated by cool (T$_{\rm eff}$ <9,000 K) objects.

Regarding the mass distribution (bottom panel of Fig.3) the *Gaia* white dwarf sample shows a bimodal-like distribution which is not present in the simulated sample. The excess of massive white dwarfs presented by the observed sample is linked to the characteristic bifurcation shown in the magnitude-color diagram (see Fig.2). Possible discrepancies between DA and non-DA cooling tracks do not seem to be plausible explanations for this observed bifurcation and excess of massive white dwarfs. A detailed analysis of the magnitude-color and color-color diagrams reveals that no more than $\approx 30-40\%$ of the objects belonging to the bifurcation region may be non-DA white dwarfs (see Fig. 6 from Jiménez-Esteban et al. (2018) and discussion therein). Although white dwarf atmosphere models for non-DA stars, such as DZ, DQ or DAB, need to be more deeply studied, alternative explanations such as white dwarf binary mergers, bursts of star formation, or alternative initial-to-final mass relations should also be taken into account.

A preliminary exercise in order to estimate the contribution of white dwarf mergers has been performed. We expand our population synthesis code by including binary stellar systems. We use the binary stellar evolution code BSE (Hurley et al., 2000) to evolve the binary systems we generate in our population synthesis model as first presented in Camacho et al. (2014) and further developed by Cojocaru et al. (2017). Our first trial consists in a standard model with a binary fraction of $f_{\rm bin} = 0.80$, a common-envelope parameter value of $\alpha_{\rm CE} = 0.1$ and internal energy $\alpha_{\rm int} = 0.1$, and a flat initial mass ratio distribution, $n(q) = 1$. The corresponding mass distribution is shown in the top panel of Fig.4 as a red open histogram compared to the observed mass distribution (gray histogram). Although the high binary fraction value adopted, it seems not enough to reproduce the observed excess of massive white dwarfs. A second model has been proved with a standard binary fraction $f_{\rm bin} = 0.50$ a common-envelope parameters of $\alpha_{\rm CE} = 0.3$ and $\alpha_{\rm int} = 0$ but, in this case, we adopt the hypothesis that the mass of the white dwarf merger follows a Gaussian distribution centered a $0.8\,M_{\odot}$ and with a dispersion of $0.1\,M_{\odot}$. The corresponding mass distribution for this model is shown in the bottom panel of Fig.4. As can be seen, in this case the simulated sample reproduce the excess of massive white dwarfs, although a slight shift is presented in the peak of the distribution.

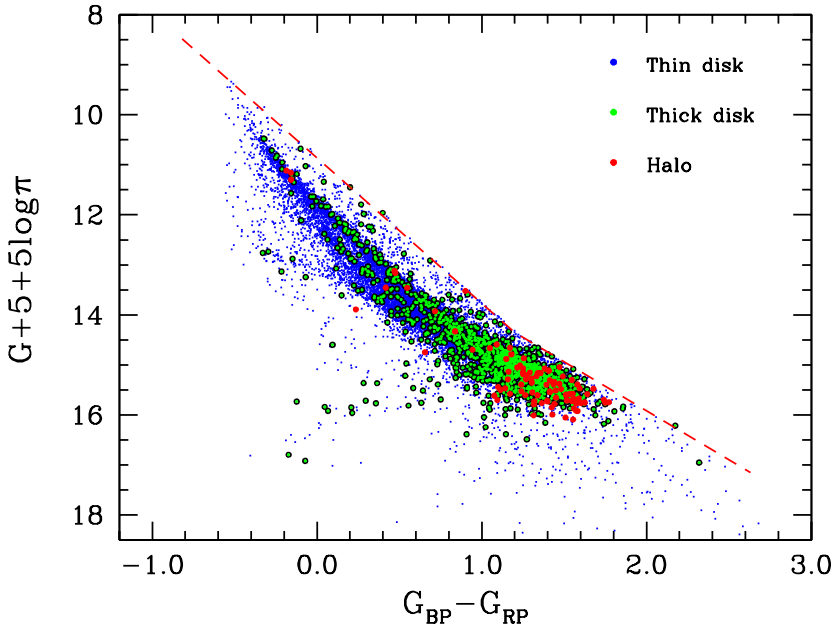

Figure 5: Color-magnitude diagram for the 100 pc *Gaia* sample as resulting after applying our Random Forest classification algorithm. The three Galactic components have been disentangled, obtaining 12,227, 1,410 and 97 white dwarf candidates for the thin and thick disk, and halo, respectively.

4 Identifying the Galactic Components

The huge quantity along with the high quality of the photometric and astrometric data provided by *Gaia*-DR2 permit us to deeply analyze the white dwarf kinematic and their main evolutionary characteristics. On the other hand, recent advanced in artificial intelligent algorithms permit us to study their main population properties in order to disentangle the different components of the Galaxy, i.e., thin and thick disk and halo. We briefly describe here our main preliminary results, while a full description of the classification method and a complete discussion of the results will be provided in a forthcoming paper.

The Artificial Intelligent method used in our study is a Random Forest algorithm widely used for classification purpose (Breiman, 2001). It is a supervised method in the sense that a initial labeled sample is needed to train the algorithm. Once trained, the algorithm is tested in the initial labeled sample and then applied to the sample that we want to classify. Our synthetic population sample is used by the algorithm in the training and testing stages. The Random Forest algorithm is applied to a 10-dimensional space formed by the equatorial coordinates, proper motion coordinates, μ_α^* and μ_δ, parallax, pass-bands G, $G_{\rm BP}$ and $G_{\rm RP}$ and also added the tangential velocity and the reduced proper motion, $H_{\rm G} = G + 5\log\mu + 5$. This expanded 10-dimensional space permit the algorithm to maximize the information in order to classify its different components.

Our preliminary results show that the algorithm presents a 86% of reliability when tested in our synthetic sample. This score is higher than the 80% presented by the reduced proper motion criteria usually applied for selecting different kinematic populations. When applied to the whole *Gaia* 100 pc sample (that is to say, all white dwarfs within 100 pc without restriction in colors) our Random Forest algorithm find 12,227 thin disk, 1,410 thick disk and 97 halo white dwarf candidates. These values represent the 89%, 10% and 1% of the whole population and imply a numerical spatial density of $4.4 \pm 0.4 \times 10^{-3}\,{\rm pc}^{-3}$, $4.9 \pm 0.4 \times 10^{-4}\,{\rm pc}^{-3}$ and $4.8 \pm 0.4 \times 10^{-5}\,{\rm pc}^{-3}$, respectively. However, for absolute G magnitudes in the range, $15 < M_G < 16$ the thin disk contribution is reduced to a 65%, while the thick disk and halo increase to a 32% and 3%, respectively. The corresponding location of the white dwarf Galactic components in the color-magnitude diagram is shown in Figure 5.

Our Random Forest algorithm is also able to disentangle the different Galactic components even if there is an overlap in the distribution. This would be not the case if only the reduced proper motion criterion was used. The corresponding tangential velocity distributions obtained by our algorithm are shown in Figure 6. In view of Fig.5 and Fig.6 we clearly identify halo white dwarf candidates as an old and high velocity population, while the thin disk population, which represent the vast majority of the 100 pc *Gaia* white dwarf population, follows a scale height distribution with $H = 200$ pc.

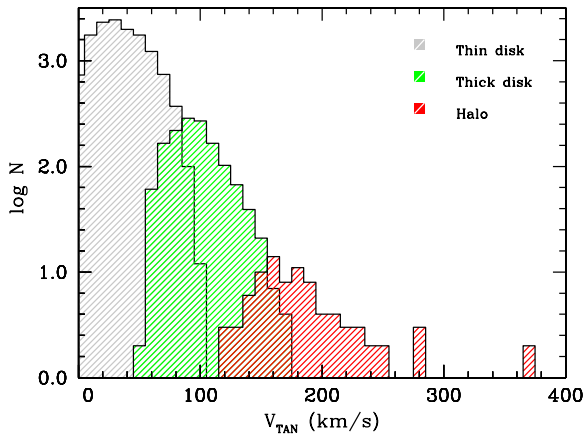

Figure 6: Tangential velocity distribution for the thin disk (gray histogram), thick disk (green histogram) and halo (red histogram). Our Random Forest algorithm allows unraveling the different Galactic components even if there is an overlap in the distribution.

5 Conclusions

Gaia Data Release 2 has provided a wealth of unprecedented information for the local white dwarf population. With the aid of a detailed Monte Carlo simulator we built a thorough population synthesis model of the thin disc, thick disc, and halo white dwarf population of our Galaxy. This fact together with the high quality of the data provided by Gaia allows to build a clean magnitude-color diagram where to select all white dwarf candidates. Our analysis shows that *Gaia* samples below 100 pc can be considered practically complete-volume samples, while above this distance magnitude-selection effects shall be taken into account.

With the use the Virtual Observatory tool VOSA we derive effective temperatures and luminosities for our sources by fitting their spectral energy distributions. In particular, we analyze 8,343 CO-core and 212 ONe-core white dwarf candidates within $-0.52 < (G_{\rm BP} - G_{\rm RP}) < 0.80$, deriving their effective temperatures, luminosities, stellar radii and masses. The *Gaia* 100 pc white dwarf population is clearly dominated by cool ($\sim$8,000 K) objects and reveals a significant population of massive ($M \sim 0.8 M_{\odot}$) white dwarfs, of which no more than $\sim 30 - 40\,\%$ can be attributed to hydrogen-deficient atmospheres. Preliminary results including white dwarf mergers for standard assumptions of binary stellar evolution models are not enough to explain this excess of massive stars. In order to be able to reproduce the observed mass distribution, we need to assume some *ad hoc* hypothesis, in particular, that the mass of white dwarf merger is centered at $0.8 \pm 0.1\,M_{\odot}$. Finally, we use an Intelligent Artificial method based on the Random Forest algorithm to disentangle the different Galactic components of the white dwarf population. With the aid of our population synthesis sample, the algorithm is trained and tested, achieving a 86% of reliability, higher than the reduced proper motion criteria. Our results show that the thin disk, thick disk and halo ratio in the 100 pc sample is 89:11:1. The thin disk population presents a spatial density of $4.4 \pm 0.4 \times 10^{-3}\,{\rm pc}^{-3}$ and clearly follows a scale height distribution with $H = 200$ pc. The algorithm also identified 97 old and high kinematic objects, clearly belonging to a halo white dwarf population.

References

Althaus L. G., Camisassa M. E., Miller Bertolami M. M., Córsico A. H., García-Berro E., 2015, A&A, 576, A9

Bayo A., Rodrigo C., Barrado y Navascués D., Solano E., Gutiérrez R., Morales-Calderón M., Allard F., 2008, A&A, 492, 277

Breiman L., 2001, Kluwer Academic Publishers., 45, 5

Camacho J., Torres S., García-Berro E., Zorotovic M., Schreiber M. R., Rebassa-Mansergas A., Nebot Gómez-Morán A., Gänsicke B. T., 2014, A&A, 566, A86

Camisassa M. E., Althaus L. G., Rohrmann R. D., García-Berro E., Torres S., Córsico A. H., Wachlin F. C., 2017, ApJ, 839, 11

Cojocaru R., Rebassa-Mansergas A., Torres S., García-Berro E., 2017, MNRAS, 470, 1442

García-Berro E. Torres S., Isern J., Burkert A., 1999, MNRAS, 302, 173

García-Berro E., et al., 2010, Nature, 465, 194

Hurley J. R., Pols O. R., Tout C. A., 2000, MNRAS, 315, 543

Jiménez-Esteban F. M., Torres S., Rebassa-Mansergas A., Skorobogatov G., Solano E., Cantero C., Rodrigo C., 2018, Monthly Notices of the Royal Astronomical Society, 480, 4505

Koester D., 2010, Mem. Soc. Astron. Italiana, 81, 921

Renedo I., Althaus L. G., Miller Bertolami M. M., Romero A. D., Córsico A. H., Rohrmann R. D., García-Berro E., 2010, ApJ, 717, 183

Rowell N., Hambly N. C., 2011, MNRAS, 417, 93

Torres S., García-Berro E., 2016, A&A, 588, A35

Torres S., García-Berro E., Burkert A., Isern J., 2001, MNRAS, 328, 492

Torres S., García-Berro E., Isern J., Figueras F., 2005, MNRAS, 360, 1381

Torres S., García-Berro E., Althaus L. G., Camisassa M. E., 2015, A&A, 581, A90